Navigation of the Mariner 10 Spacecraft to Venus and Mercury

Carl S. Christensen* and Stephen J. Reinbold†
Jet Propulsion Laboratory, Pasadena, Calif.

Orbit determination techniques used during the highly successful flight of Mariner 10 to Venus and Mercury are presented. Comparisons are made between different data sets, different sets of parameters, and between a conventional least squares batch filter and a sequential batch filter and smoother that was designed for this mission. The sequential filter was able to account for small spacecraft forces that the batch filter was unable to handle effectively, and hence, contributed greatly to the mission success. The sequential filter and smoother design is given as well as results for each phase of the mission.

I. Introduction

AT the present time, the Mariner 10 spacecraft is on its way towards a third encounter with Mercury in March, after highly successful Mercury encounters in March and September 1974 in which all scientific objectives were met or exceeded.‡ Mariner 10 was the first spacecraft to successfully flyby two planets, using the "gravity assist" of the first to aim towards the second. As such it was highly dependent on precise navigation.

The success of the navigation is illustrated by the Venus flyby only seventeen kilometers from the desired aim point. This allowed a successful Mercury encounter with a restricted maneuver and allowed the possibility of multiple Mercury encounters. This paper will discuss the orbit determination (OD) techniques and results for each phase of the mission.

II. Preliminaries

A. Orbit Determination Software

Orbit determination was done with two filters: 1) a classical least-squares "batch filter", and 2) a batch "sequential" filter and smoother. The batch filter has been the standard tool for orbit determination for interplanetary missions. This mission was the first to extensively use a sequential filter and smoother. This filter was designed to be implemented specifically for use in the Mariner 10 Mission. It is a square root information filter with these characteristics:

1) The data arc is divided into "batches" usually one day. Stochastic parameters are modeled as piecewise constant functions; i.e., they are constant during each batch. They are exponentially correlated between batches. In other words,

$$E(\rho_i) = e^{\frac{-\Delta t}{\tau}} \rho_{i-1}$$

where ρ_i is a stochastic parameter for the ith batch, ρ_{i-1} is the determined value for the $i-1$ st batch, Δt is the batch size, τ is the correlation time, and $E(\ )$ is the expected value.

2) A parameter can be treated as both deterministic and stochastic. This means that the filter can estimate both a bias and a random fluctuation about the bias value.

3) Estimates and covariances can be mapped with process noise. In other words the a priori values for the stochastic parameters are included in the mapping.

4) Efficient smoothed residuals are available.

The basic equation for the filter and smoother are given in Ref. 1. Reference 2 gives a good exposition of square root filtering and smoothing.

In preparation for this mission an additional important change was made to the OD software. A complex solar pressure model was implemented in order to account for articulating solar panels and high gain antenna. The solar panels were tilted many times during the mission and the high gain antenna remained pointed at the earth. The model was quite successful in simulating the varying forces involved.

B. Orbit Determination Strategy

1. Data

Tracking data was essentially continuous from launch through the first Mercury encounter. The data was taken at six different Deep Space Net (DSN) stations—26 and 64 m antennas at Goldstone, California, Madrid, Spain, and Canberra, Australia.

The primary data type was two-way Doppler taken at a nominal 60 sec sample rate. This data was edited and compressed to a count time of 600 or 1200 sec. The two overseas 26 m stations obtained near-Earth ranging data (MARKIA) for the first 2 months of the mission. This was selected at 600 or 1200 sec. The remaining stations had planetary ranging systems that produced one to three points per pass when active.

Throughout the flight, solutions were computed using three data sets; Doppler only, Doppler and range, and range only. Consistency among the solutions increased confidence in the data. Normally, the Doppler and range solutions were the ones in which most confidence was placed.

2. Solution Sets

The frequency of OD solutions ranged from one per week during cruise periods to once every hour or two during launch and encounter periods. Each OD solution was in reality a large set of solutions consisting of batch filter runs estimating: a) the spacecraft state; b) state + station locations; c) state + solar pressure; d) state + attitude control forces; e) state + station locations + solar pressure; f) same as (e) + attitude control; and g) all parameters and sequential filter runs duplicating all but (d) and (f). The attitude control forces,i.e., spacecraft accelerations along the three spacecraft axes were used as stochastic parameters in all of the sequential filter runs. Parameters in (g) include all those mentioned plus planetary, Earth, and moon masses and ephemerides depending on the mission phase. The sequential filter was run with stochastic attitude control acceleration a

Presented as Paper 74-844 at the AIAA Mechanics and Control of Flight Conference, Anaheim, California, August 5-9, 1974; submitted September 27, 1974; revision received January 27, 1974. This paper presents the results of one phase of research carried out at the Jet Propulsion Laboratory under Contract NAS 7-100, sponsored by NASA.

Index categories: Spacecraft Navigation, Guidance, and Flight-Path Control Systems; Spacecraft Tracking.

*Member of the Technical Staff.

†Engineer.

‡Since this paper was written Mariner 10 had a third successful Mercury encounter on March 21, 1975. It died a week later with depletion of the attitude control gas.

priori sigmas of 10^{-12} km/sec^2 or 10^{-11} km/sec^2. A batch size of one day and correlation time of from 1-5 days.

C. The *B*-plane

Planetary targeting is usually expressed in terms of the "*B*-plane." The *B*-plane is a plane passing through the center of a target planet perpendicular to the incoming asymptote of a spacecraft. $B\cdot T$ is the intersection of the *B*-plane with the ecliptic, and $B\cdot R$ is a vector in the *B*-plane perpendicular to $B\cdot T$ in the negative declination direction.

III. The Flight from Earth to Venus to Mercury

Figure 1 shows the flight path of Mariner 10 from launch through the first Mercury encounter. Four trajectory correction maneuvers (TCMs) were planned, two between Earth and Venus, and two between Venus and Mercury. The first two were carried out as planned. TCM_1 was executed on 13 November to correct the errors induced at launch. TCM_2 was a much smaller maneuver on January 18 to correct the error induced by TCM_1 and early orbit determination errors. The two maneuvers between Venus and Mercury were replaced by a single maneuver on March 16.

On January 28, one week before Venus encounter, the spacecraft developed a serious problem. The roll gyros began oscillating at a rapid rate, causing the roll position jets to fire at their maximum rates. The immediate effect was large consumption of cold nitrogen used as attitude control gas (1.2 lb in 80 min) before the problem was diagnosed and the gyros turned off. The thrust imbalance in the attitude control jets imparted a force on the spacecraft causing an average acceleration of about $1.79+10^{-9}$ km/sec^2 for the 80 minutes. Another spacecraft acceleration occurred on February 14, when the gyros were turned on in order to test the conditions under which the January 28 failure had occurred.

For orbit determination, the large accelerations over short time periods as in the TCMs and in the two events on January 28 and February 14 are best treated as instantaneous velocity changes. When such a velocity change is within a data arc used for an OD fit, the velocity changes tend to absorb errors and no more information is gained than that from two OD fits, one before and one after the ΔV. For that reason OD fits were made only over data arcs where there were no sudden, large accelerations. Figure 2 shows the six time spans where OD fits were made: A-launch to TCM_1, B-TCM_1 to TCM_2, C-TCM_2 to January 28, D-January 28 to February 14, E-February 14 to TCM_3, and F-TCM_3 through Mercury encounter.

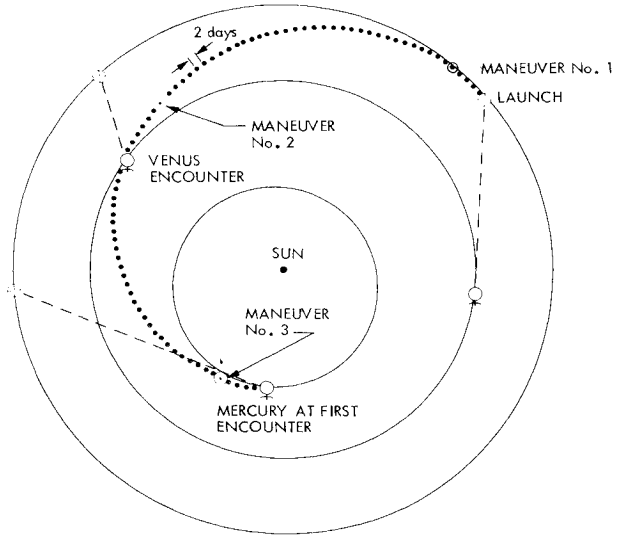

Fig. 1 Projection of the Earth to Mercury trajectory into the ecliptic plane.

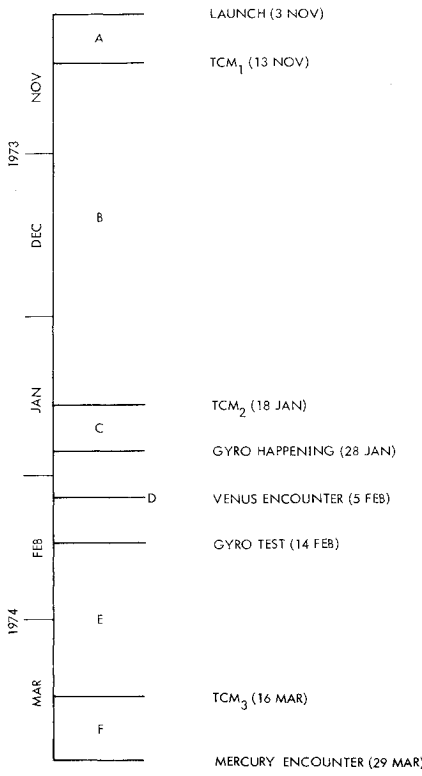

Fig. 2 Timeline from launch to Mercury I.

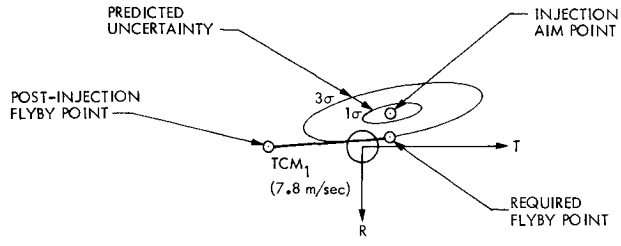

POST INJECTION B-PLANE CONDITIONS

VENUS CONDITION	AIM POINT	ACHIEVED
B•T, km	16,150	-51,300
B•R, km	-17,500	-180
TIME OF CLOSEST APPROACH	2/5/74 $17^h\ 20^m$	2/5/74 $20^h\ 13^m$

Fig. 3 Injection results in the Venus *B*-plane.

A. Launch to TCM_1

When the spacecraft is within the strong gravity field of the Earth, its orbit can be determined rather quickly compared to the time required in interplanetary space. One day after launch when tracking stations around the Earth had supplied tracking data, a reasonable OD was obtained. This fit was updated over the next few days and used to plan TCM_1 at launch plus 10 days.

Figure 3 shows in the Venus *B*-plane the post launch trajectory and the TCM_1 correction need to change the trajectory to go through the aim point.

Using Doppler and range data the one sigma error ellipse was about 400 km by 200 km. This is small compared to the TCM_1 execution one sigma error of 1500 km. The batch filter and sequential filter performance was similar in this phase due to the strong near Earth data and the short time span.

B. TCM_1 to TCM_2

This mission phase was the most critical for orbit determination. The accuracy of the orbit determined the parameters for TCM_2 which in turn determined the Venus

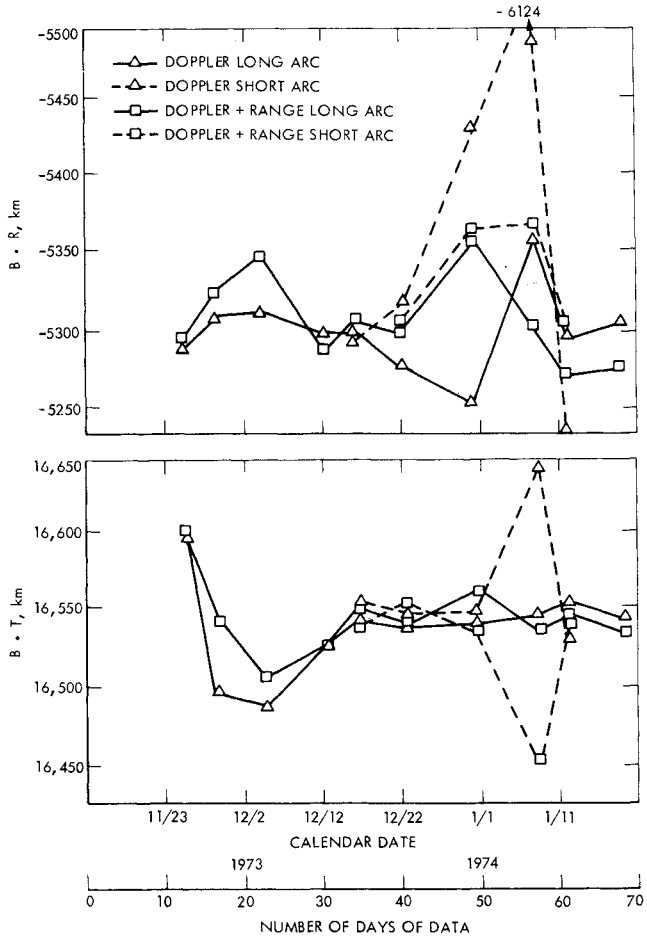

Fig. 4 Time history of solutions in the Venus *B*-plane—batch filter.

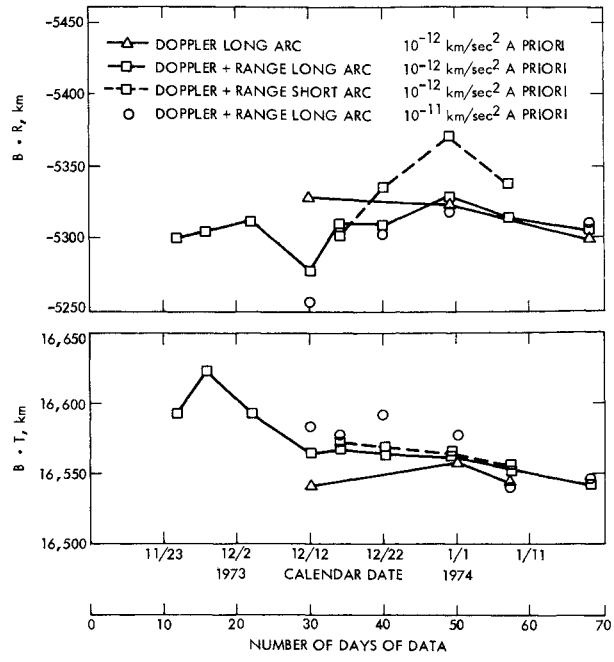

Fig. 5 Time history of solutions in the Venus *B*-plane—sequential filter.

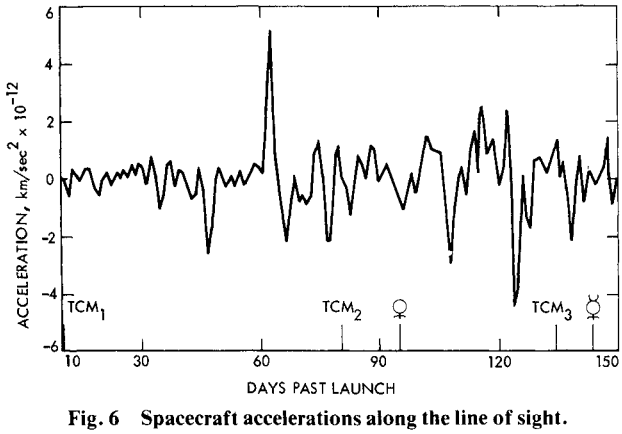

Fig. 6 Spacecraft accelerations along the line of sight.

delivery accuracy. Due to the geometry of the swingby trajectory there was a 1 to 1000 mapping of errors from Venus to Mercury. In other words, a 1 km miss at Venus mapped into a 1000 km miss at Mercury.

A time history of solutions in the Venus B plane is shown in Fig. 4 for batch filter solutions, and Fig. 5 for sequential filter solutions. Solutions for both long and short data arcs are shown for Doppler only and Doppler + range. The long data arc is from TCM_1 (11/13) to the data shown on the abcissa. The short data arc is the 20 days preceding the date shown on the abscissa. All solutions shown include the spacecraft state, solar pressure parameters, and station locations. This solution set was chosen as most representative; other solution sets show similar behavior. Note that all of the fits with data up to Dec. 24 showed good agreement. The batch filter fits with data up to Jan. 2, however, show a wide scatter in $\boldsymbol{B}\cdot\boldsymbol{R}$. One week later with data up to Jan. 10 the wide scatter is apparent in both $\boldsymbol{B}\cdot\boldsymbol{R}$ and $\boldsymbol{B}\cdot\boldsymbol{T}$ with the short arc Doppler solution 800 km high in $\boldsymbol{B}\cdot\boldsymbol{R}$. The sequential filter, on the other hand, with the exception of a short arc solution high in $\boldsymbol{B}\cdot\boldsymbol{R}$, remained remarkably flat throughout the entire time period.

In addition to the scatter of solutions the data residuals showed a very small trend starting about January 4. The stochastic acceleration solution from the sequential filter and smoother showed a comparatively large (about 5×10^{-12} km/sec^2) acceleration on January 4. Subsequent analysis of telemetered limit cycle data confirmed that there were unusual spacecraft forces for a 25 hour period. Figure 6 shows a plot of the spacecraft accelerations along the Earth-S/C line of sight as determined by the sequential filter. The January 4 (60 days) acceleration is the first large positive peak.

The performance of the sequential filter as shown in Fig. 6 and its ability to determine S/C accelerations was impressive. Its use gave a high degree of confidence to the solution used to define the parameters for TCM_2.

C. TCM_2 to January 28

After TCM_2 OD solutions were made every two days in order to get a rapid determination of the trajectory. Had TCM_2 not been successful there was still time to do another maneuver prior to Venus encounter. Here the batch and sequential filter gave similar results over the one week period. Figure 7a shows the solutions in the Venus *B*-plane for 3, 5, and 7-day arcs.

D. Near Venus

After the gas acceleration on January 28, short arc fits were again made every two days. Figure 7b shows these solutions for 3, 5, and 7 days. Also shown is the actual trajectory point determined after the Venus flyby. By comparing these solutions with those of the previous week, it is seen that the January 28 acceleration moved the trajectory about 15 km in the *B*-plane. This number is consistent with that obtained by solving for the acceleration and analyzing the spacecraft telemetry giving gas usage and torques. Due to the large Venus gravity field experienced approaching and leaving the planet, the state of the spacecraft was determined very accurately (< 1 km in the Venus *B*-plane). A 1 km error at Venus maps to a 1000-km error at Mercury.

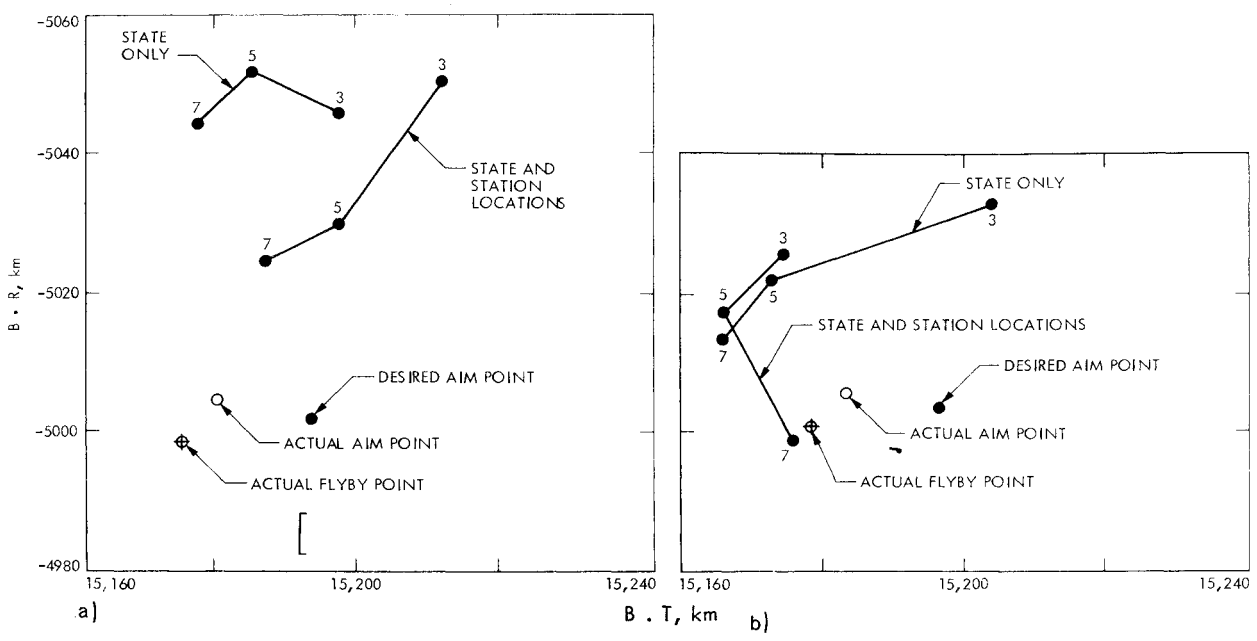

Fig. 7 Venus approach short arc solutions. a) before Jan. 28, b) after Jan. 28.

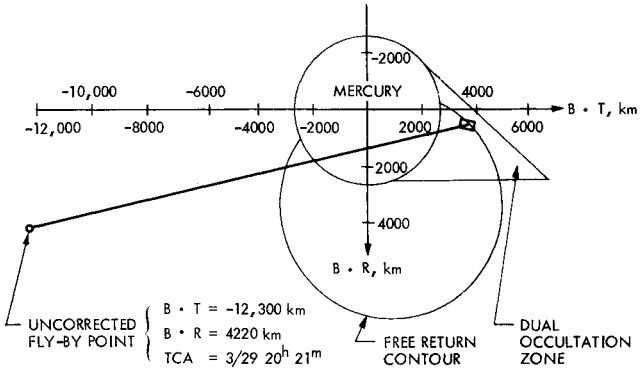

Fig. 8 Post Venus trajectory mapped to the Mercury B-plane.

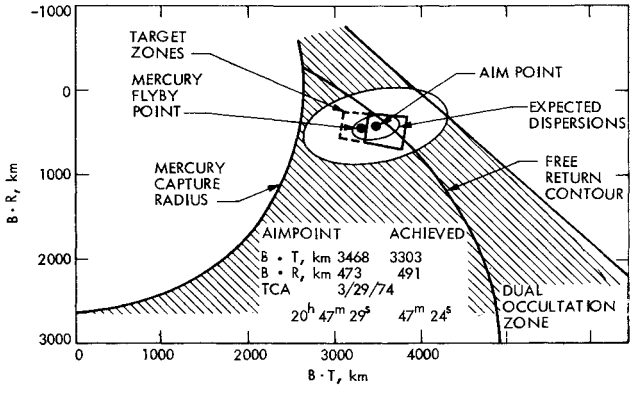

Fig. 10 Mercury I flyby.

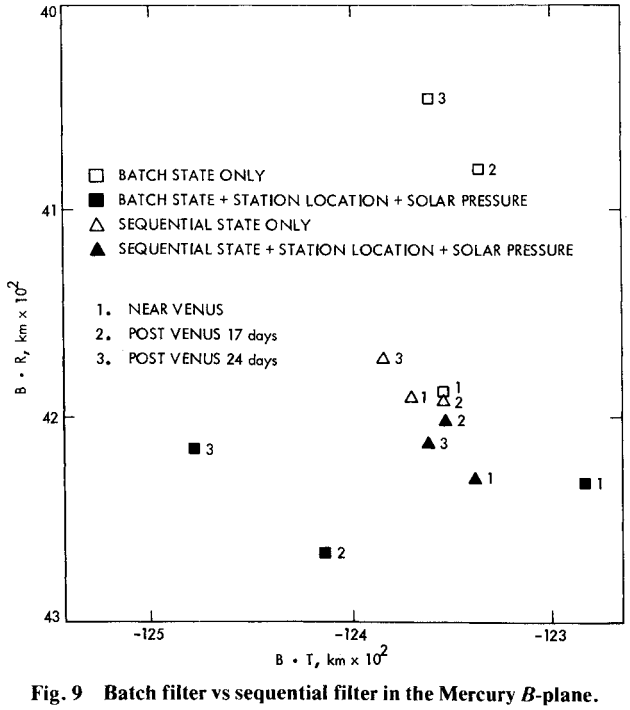

Fig. 9 Batch filter vs sequential filter in the Mercury B-plane.

Figure 8 shows the Mercury B-plane with the aim zone and the uncorrected flyby point given the Venus solution. The one sigma error ellipse is about 400 km by 150 km.

E. February 14 to TCM_3

After the gyros were turned on in a testing mode on February 14, it was decided to not attempt a full maneuver where the gyros would be on for an hour or so. Instead a "sunline" maneuver in which there are no turns, and the gyros need only be on for the duration of the engine firing was performed. The engine nozzle points towards the sun on the spacecraft, so the thrust vector imparted to the spacecraft is along the sun-S/C line, hence the name "sunline." Rather than three degrees of freedom, the sunline maneuver only has two, the magnitude of the thrust and the time the maneuver takes place. The trajectory was such that the desired aim point could be achieved with a TCM on March 16.

The orbit determination during this phase and the maneuver errors at TCM_3 determined the Mercury delivery accuracy. Again the sequential filter solutions showed more stability than the batch solutions. This is shown in Fig. 9 where the near Venus and the later sequential filter solutions are seen to agree quite well.

F. TCM_3 to Mercury

The primary purpose of orbit determination during this phase was to accurately determine the trajectory so that the

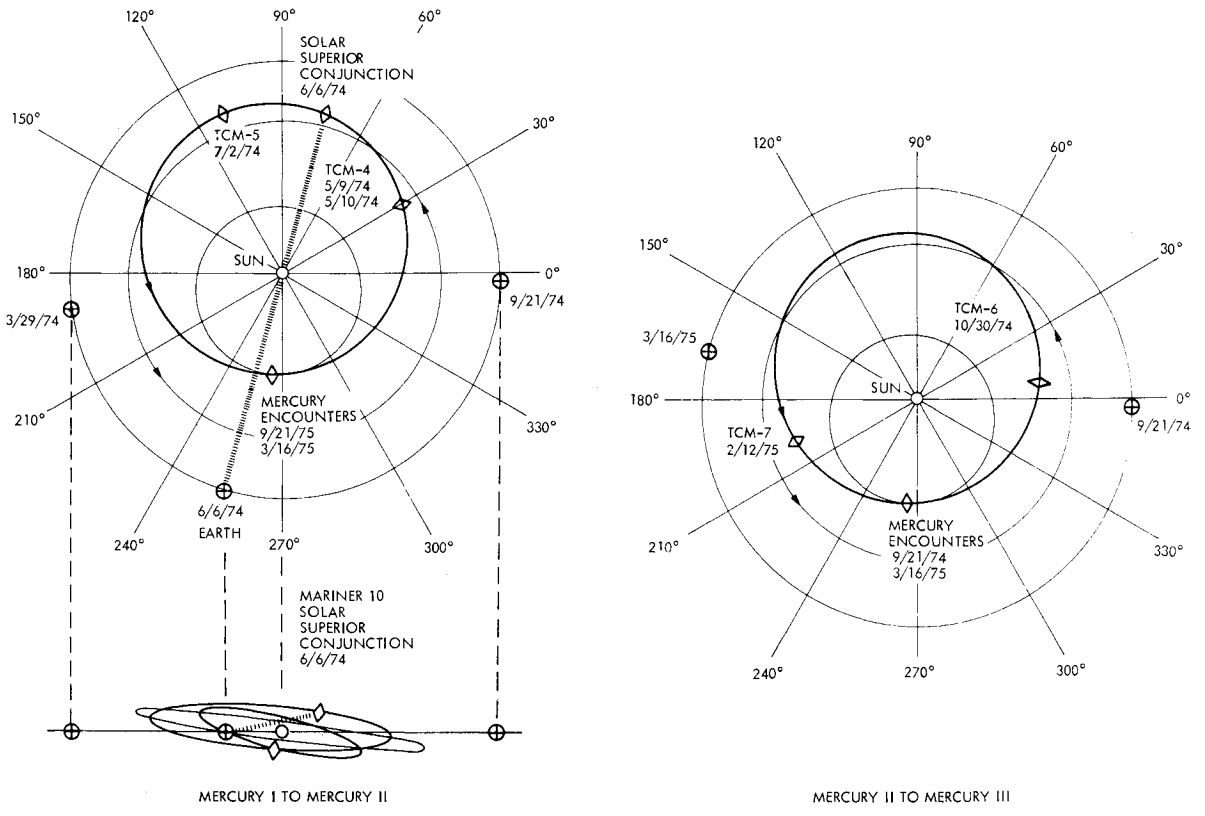

Fig. 11 Significant events: Mercury I to Mercury III.

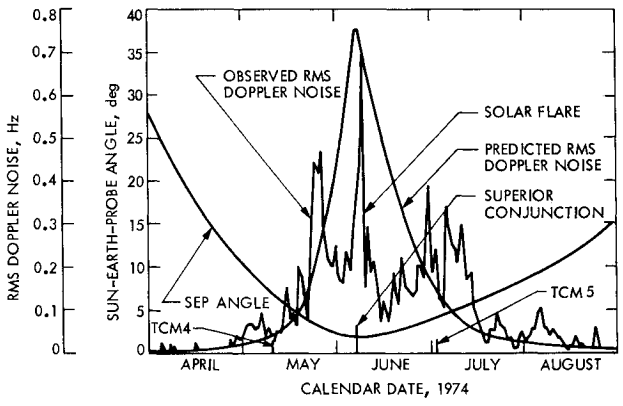

Fig. 12 Doppler noise vs the sun-Earth-probe angle.

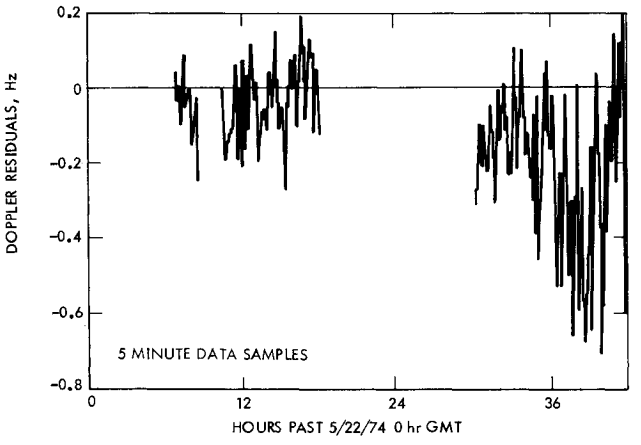

Fig. 13 Doppler noise and signatures from data near superior conjunction.

science instruments could be pointed accurately. As the spacecraft passed close to the planet, again the trajectory was determined very well with respect to Mercury (2km). Figure 10 shows the Mercury flyby point in the *B*-plane. It was 160 km from the aim point within the aim zone and about 250 km from the free return contour.

IV. The Extended Mission—Mercury II and Mercury III

Following the highly successful Mercury I encounter activities, thoughts were turned to the possibility of Mercury II. An Orbit Determination Study was performed to determine the Mercury II *B*-plane uncertainties for the two maneuvers needed to put the spacecraft on a "bright side" Mercury II flyby. Based on the results of these studies and some very efficient maneuver analysis, it was determined that a dark side Mercury III pass could also be obtained, providing the spacecraft attitude control gas was utilized efficiently. Also occurring during this period is a superior conjunction with the spacecraft passing within 6.25 solar radii.

Figure 11 presents the Mercury I to Mercury II and Mercury II to Mercury III flight path. Shown on this figure are the five planned maneuvers (TCM_{4A}, TCM_{4B}, and TCM_5 have been performed), time of superior conjunction and the Mercury II and Mercury III encounters.

A. Data Quality During Superior Conjunction

It is expected that when a radio signal passes through the solar corona that it will be affected by the charged particles present there much in the same way that a radio signal passing through the earth's ionosphere is affected. The amount of perturbation is directly related to the sun-Earth-probe angle (SEP) by a $1/R^4$ relationship where R is the sun-radio signal distance. The sun's corona is thought to extend to a *SEP* angle of about 4°.

Figure 12 shows the *SEP* angle plotted as a function of time. Also plotted is the expected 1σ data noise for a 1-min. Doppler sample as a function of *SEP* angle from the results of the Mariner 9 superior conjunction. In like manner the

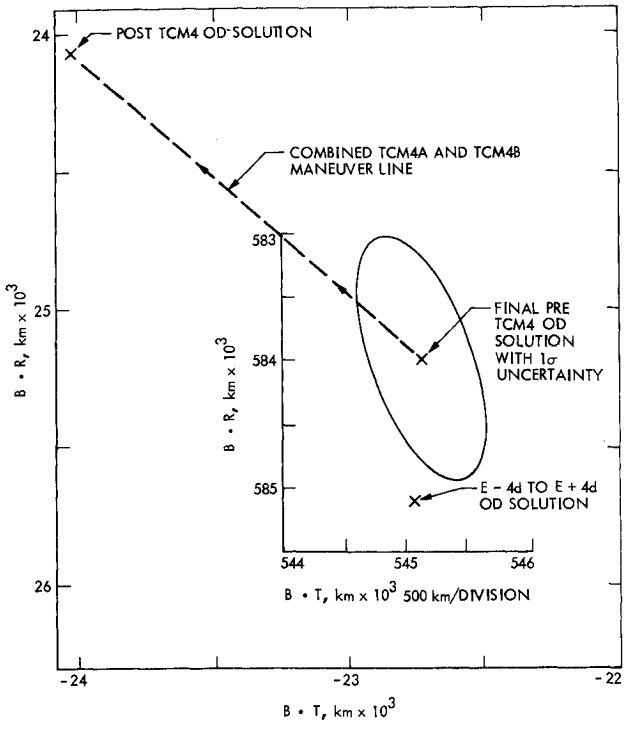

Fig. 14 TCM_4 shown in the Mercury II B-plane.

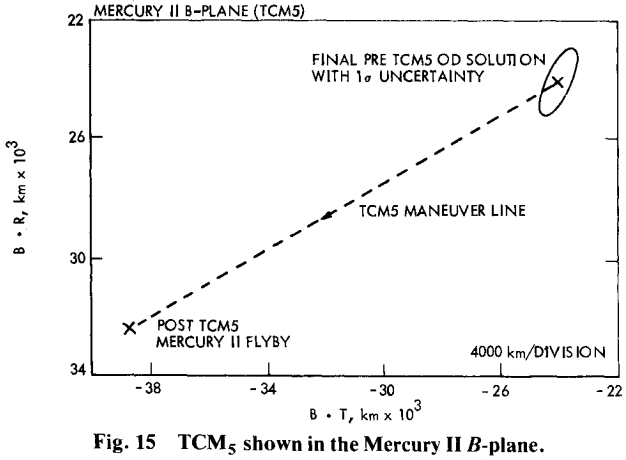

Fig. 15 TCM_5 shown in the Mercury II B-plane.

realized rms data noise from the Mariner 10 conjunction is plotted. The rms noise of the Mariner 10 radio signal has followed the expected curve quite well except that the peak noise was not reached. This is due to a stronger earth received radio signal because the Mariner 10 Earth-S/C distance is 2.6×10^8 km while that of Mariner 9 was 4.0×10^8 km at superior conjunction. The data noise is a direct function of received signal strength at the DSS tracking stations.

At about the same time that the data noise started to increase, large signatures started appearing in the data. The magnitude of these signatures varied from day to day but in general increased as the *SEP* angle became smaller. Figure 13 shows Doppler data for two adjacent days. The fluctuation in the noise and signatures is quite apparent. The Doppler noise of the second day is 50 times greater than that of a radio signal from the same Earth-probe distance not affected by the sun.

B. Mercury I to TCM_4

This phase of the mission is nominally an excellent time for orbit determination. The large acceleration resulting from the flyby of a large body (Mercury) is a helpful aid to determining the spacecraft position and velocity. Three separate strategies

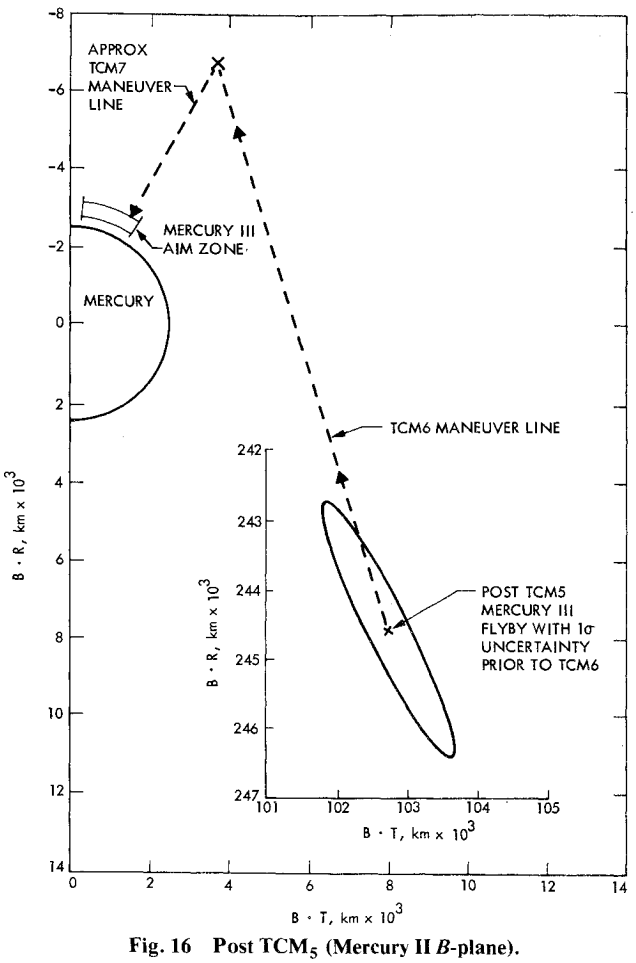

Fig. 16 Post TCM_5 (Mercury II B-plane).

were tried; data were fit from 1) Em-4d to Em+4d; 2)Em +1 hr to latest data available (eventually to TCM_4); and 3) Em + 2d to latest data available.

The third strategy soon was eliminated. With the increased data noise and signatures, the B-plane solution spread became greater as more data were added.

The first strategy gave very consistant B-plane results between various data-type solutions 1) Doppler data only; and 2) Doppler plus range data. There were also consistent solutions between the batch and sequential filters. The final solution based on this strategy had the following parameters in the Mercury II B-plane: $\boldsymbol{B}\cdot\boldsymbol{R}=585{,}089$ km, $\boldsymbol{B}\cdot\boldsymbol{T}=545{,}119$ km, and TCA = 9/19/74 20/hr 4/min 1/sec.

The second strategy proved to also have very consistent solutions between data types and filters. The final B-plane solution mapping was $\boldsymbol{B}\cdot\boldsymbol{R}=583{,}978$ km, $B\cdot T=545{,}119$ km, and TCA = 9/19/74 20/hr 5/min 46/sec.

Figure 14 presents the solutions along with the one sigma SMAA on the solution used for TCM_4. Also shown are the results of the TCM_4 maneuver (performed in two parts due to S/C thermal constraints) in the Mercury II B-plane. These solutions disagreed by 780 km in the B direction which was small compared to 1σ maneuver uncertainties of 10000 km. The solution chosen for TCM_4 was from the second strategy. This choice was governed by the following rationale; the first strategy has the following B-plane uncertainties; 1) a 1-km uncertainty in the Mercury I B-plane, 2) $\boldsymbol{B}\cdot\boldsymbol{R}$ in the Mercury I B-plane had a 1σ uncertainty of 2 km and 3) the program computed 1σ uncertainty was on the order of 5000 km in the Mercury II B-plane.

C. TCM_4 to TCM_5

This phase had several significant events. The most important item was the decision to go to the bright side at Mer-

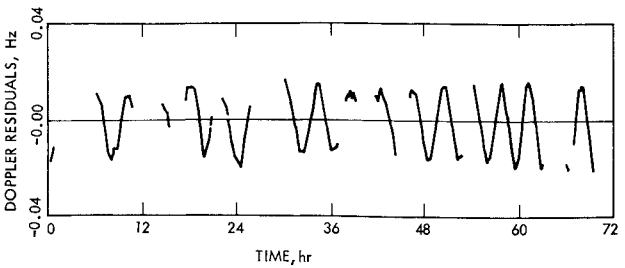

Fig. 17 Two-way-Doppler roll residuals.

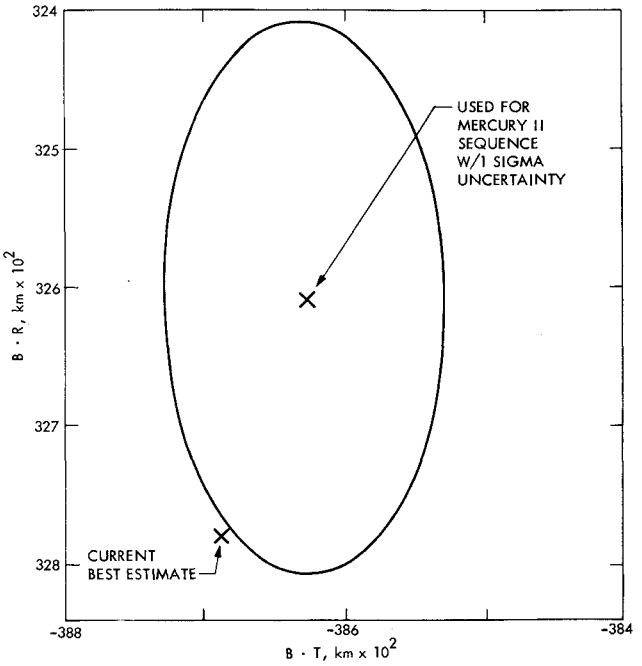

Fig. 18 TCM_6 shown in the Mercury III *B*-plane.

cury II which would allow a good probability for a dark side Mercury III. The bright side Mercury II is excellent for TV whereas the dark side Mercury III is excellent for celestial mechanics and the magnetic field experiment and good for TV. Superior conjunction occurred midway through this phase with the resultant high data noise and data signatures corrupting the orbit determination data as previously discussed.

Figure 15 presents the solution for this phase along with its associated 1σ uncertainty and also shows the TCM_5 maneuver which has put the S/C at an approximate *B* distance of 50,000 km.

D. TCM_5 to Mercury II

This was a cruise portion of the mission, relatively uneventful for orbit determination. The OD function during this period was to determine the orbit with sufficient accuracy for TV pointing during the Mercury II encounter sequence.

Figure 16 presents the post-TCM_5 solution in the Mercury II *B*-plane used for the Mercury II sequence with its 1σ OD uncertainty and the actual flyby point determined post-Mercury II.

E. Mercury II and Mercury III

This segment of the mission was designed as a close, dark side Mercury II pass to be mainly utilized by the magnetic field and celestial mechanics experiments with two (possibly three) planned maneuvers required to put the spacecraft on the required course.

Unexpected loss of the already short attitude control gas forced the project into putting the spacecraft into a roll drift mode on October 4, 1974 with the roll rate controlled by "solar sailing" using the articulating solar panels and high gain antenna as "sails." Figure 17 presents a sample of the roll signature in the Doppler residuals over a 2-day period. Since the period of the roll is relatively short (4-12 hr), the tangential forces due to solar pressure are nullified. This necessitated changes to existing software and creation of software to model the signature.

TCM_6 was performed on October 30, 1974 and put the spacecraft on a dark side Mercury II trajectory. TCM_7 will be performed on February 12, 1975 to put the spacecraft at an as yet undecided aim point.

Figure 18 presents the orbit solution used for TCM_6 along with its associated 1σ uncertainty. Also shown is the TCM_6 maneuver line and the Mercury II aim zone. The approximate TCM_7 maneuver line and the Mercury II aim zone are also shown.

V. Conclusions

The flight of Mariner 10 has been a most ambitious mission having completed three planetary encounters with the hope of completing one more. The navigation efforts for this mission have included some new techniques, particularly the sequential filter that have demonstrated their worth in an interesting, complex mission environment.

References

[1]Christensen, C.S., "A New DPODP Sequential Filter," MOS SRD-73-3-482/C, Nov. 1971, Jet Propulsion Laboratory, Pasadena, Calif.

[2]Bierman, G.J., "Computational Aspects of Discrete Sequential Estimation," 900-661, June 1974, Jet Propulsion Lab., Pasadena, Calif.